



Corrosion inhibition by aniline oligomers through charge transfer: a DFT approach

Lawrence T. Sein, Jr.^{a,*}, Yen Wei^b, Susan A. Jansen^a

^a Department of Chemistry, Temple University, Philadelphia, PA 19122, USA

^b Department of Chemistry, Drexel University, Philadelphia, PA 19104, USA

Received 26 February 2002; accepted 25 June 2002

Abstract

Prototype materials based on aniline oligomers have been shown to inhibit corrosion. The electronic behavior of these aniline trimers parallels that of polyaniline (PAni), but the oligomers are a much more tractable system for analysis. The anti-corrosion process involves the acid/base chemistry of the oligomers, their electron donor/acceptor properties, and the interaction of the oligomers with the metal surface.

Thermodynamic parameters for several competing reaction sequences occurring during the interaction of an iron (or aluminum) surface and aniline trimers are determined by hybrid *ab initio*/density functional theory (DFT) calculations. These parameters are used to interpret the extent of electron transfer at the polymer–surface interface at equilibrium. The rate of electron transfer from the metal to trimer, and from one trimer to another, is estimated using Marcus–Hush theory. The relevance of these rates to the corrosion process is illustrated. The pH dependence of corrosion inhibition by oligoanilines and the effect of the spin state of the oligomer is discussed.

© 2003 Published by Elsevier B.V.

Keywords: DFT; Aniline oligomers; Corrosion

1. Introduction

Polyaniline (PAni) has been widely studied for use in electrical conduction [1], electroluminescence [2], rechargeable batteries [3], and anti-corrosion applications [4]. Nevertheless, the facility of its use is restricted by its poor solubility, which makes processing more difficult. The effectiveness of its electrical conduction depends upon doping [5]. To circumvent the solubility difficulties, the focus has shifted somewhat from PAni to aniline oligomers [6], which serve as both convenient models for PAni and useful materials in their own right. Two surprising results are the demonstration that the effective conjugation length in PAni rarely exceeds three aniline units [7], and that aniline trimers are more effective than the polymer in corrosion inhibition [8].

PAni exists in three stable oxidation states, named leucoemeraldine base (LEB), emeraldine base (EB), and pernigraniline base (PB), LEB being the most reduced form, and PB the most oxidized. Similarly, the aniline

trimer can exist in three stable oxidation states, which we have named LEB **1a**, **1b**, EB **2a**, **2b**, and PB **3a**, **3b**, and hereafter all references shall be to the “trimers”, unless otherwise noted. LEB is slowly oxidized by air to EB [*N,N'*-bis(4'-aminophenyl)-1,4-quinonediimine]; the conversion of EB to LEB requires the action of phenylhydrazine in ether [8] or hydrazine sulfate in acetonitrile, followed by ammonium hydroxide [9]. EB, though stable to air oxidation, is converted to PB by hydrogen peroxide. The reverse reaction (PB to EB) is easily achieved by sodium borohydride. Each of these forms is the result of a two-electron oxidation or reduction.

The EB is easily protonated by aqueous or nonaqueous [10b,c,f and g] halogen acids, to form first the emeraldine hydrochloride **4** (ES₁), and next the emeraldine dihydrochloride **5** (ES₂). Both calculations and experiment have demonstrated that ES₂ has a paramagnetic triplet ground state, whereas all the other trimeric forms are diamagnetic ground state singlets [6c,d,7]. The salt forms are especially interesting, because corrosion inhibition seems limited to the salt forms, only the dihydrochloride is paramagnetic, and the ES forms are electron acceptors. The salt forms have only miniscule solubility in water, and the bases are completely insoluble.

* Corresponding author. Present address: School of Science and Health, Philadelphia University, Philadelphia, PA 19144, USA.
Tel.: +1-215-573-6416.

E-mail address: lsein@chemist.com (L.T. Sein, Jr.).

Phenylimines, particularly in aprotic solvents, are known to form hydrogen bonded complexes with proton donors [11]. Hydrogen bonding interactions are believed to be important in the polymer also [1f]. Since the salt form is largely insoluble (and indeed, if it were soluble in water it would hardly be a useful anti-corrosion coating), the polymer–metal interface is anhydrous (for a sufficiently thick coating of polymer). Phenylimines are so prone to the complex formation, it is likely that the ES acts more like an EB:HCl or HCl:EB:HCl complex than a conventional salt in which both the cation and ion are completely solvated. Consequently, all calculations involving ES₁ or ES₂ involve the complete complex.

2. Computational methods

The Gaussian 94 [12] suite of programs was utilized for calculations of the optimized geometries, single point energies, ionization potentials, and electron affinities of all molecules, except for those calculations utilizing the semi-empirical method ZINDO/1. Becke's three-parameter hybrid density functional B3LYP [13] was used for all molecules, except for those of the iron clusters, for which Hartree–Fock was used with the LANL2DZ effective core potential (ECP) [14]. Energies were calculated for all possible spin states of the Fe neutral cluster, and, since the high spin case was the lowest in energy, it was used as the reference for all subsequent calculations.

Ionization potentials for each molecule, M were calculated as $H(M^+) - H(M)$, and electron affinities as $H(M^-) - H(M)$. Enthalpies were determined by single point calculation at the B3LYP/6-311G(2d,p) level on a B3LYP/6-31G optimized geometry for the trimers, and B3LYP/6-31G+ [15] for the organic molecules. The presence of a true minimum was verified by inspection of the corresponding frequency calculation; zero negative frequencies confirmed a true minimum. Zero-point energies and enthalpic corrections (at 298 K) were calculated at the B3LYP/6-31G level for the trimers, and B3LYP/6-31G+ for the others, with a scaling factor of 1.00 for all. The modest 6-31G basis set was used for the trimers without polarization functions for geometry optimizations and frequency/zero-point calculations of the trimers, since earlier tests had shown that the geometries were virtually identical, and that B3LYP calculations are rather insensitive to the basis set level used for geometry optimization [16]. We therefore, decided to use the 6-31G as a prudent and efficient compromise (Tables 1, 2).

Note that ionization potentials and electron affinities were not computed by Koopmans' theorem [17].

Polarizability tensors were calculated during frequency calculations at the B3LYP/6-31G level, which has been shown to be adequate [18]. The axes are those of the *standard orientation* employed by Gaussian 94, which defined the long axis of the molecule as the x -axis, the shorter axis

Table 1
Relative energies of *syn* and *anti* aniline trimers

	H^a	μ^b	α_{zz}^c	ϵ^d
<i>syn</i> -Emeraldine 2a	−914.440270	0.001	87.30	10.0
<i>anti</i> -Emeraldine 2b	−914.440132	0.063	82.27	8.4
<i>syn</i> -Eernigraniline 3a	−913.204723	2.231	84.67	9.5
<i>anti</i> -Pernigraniline 3b	−913.205447	2.554	85.33	9.7
<i>syn</i> -Emeraldine hydrochloride 4	−1375.284411	17.772	83.85	6.5
<i>syn</i> -Emeraldine dihydrochloride (triplet) 5	−1836.102323	25.545	84.04	4.9

^a Calculated at B3LYP/6-311G(2d,p) on a B3LYP/6-31G optimized geometry. Zero-point and enthalpic corrections to 298 K at B3LYP/6-31G.

^b D^{−1}.

^c 10^{−24} cm³, as computed at B3LYP/6-31G.

^d Calculated by Clausius–Mossotti equation.

Table 2
Enthalpies of spin states of *syn* trimers^a

	S_0	T_1
Pernigraniline	−913.205447	−913.174938
Emeraldine	−914.440270	−914.440132
Emeraldine hydrochloride	−1375.284411	−1375.265902
Emeraldine Dihydrochloride	−1835.477244	−1836.102323

^a Calculated at B3LYP/6-311G(2d,p) on a RB3LYP/6-31G optimized geometry for singlet, UB3LYP/6-31G optimized geometry for triplet. Zero-point and enthalpic corrections to 298 K at R- or U-B3LYP/6-31G.

across the central ring as the y -axis, and the normal axis to the plane of central ring as the z -axis. Gaussian 94 provides both the “exact” and “approximate” polarizabilities; herein are used the “exact” *static* polarizabilities [19] (Figs. 1–5).

Semi-empirical calculations used the ZINDO/1 [20] method from within the HyperChem [21] suite of programs. The aniline trimer/metal cluster assemblies were optimized using ZINDO/1 with the metal surface constrained to crystallographic coordinates without reconstruction (Fig. 6). The constraint of the surface was achieved by setting the force constants for all bonds, bond angles, and bond torsions to be sufficiently large to prevent surface reconstruction. Earlier tests run with smaller force constants resulted in catastrophic deformations of the metal clusters, which were physically unrealistic.

The semi-empirical optimizations used a convergence limit of 0.2 kcal Å^{−1} mol^{−1} for the wavefunction, convergence being accelerated by use of the direct inversion of the iterative subspace (DIIS) method [22]. The convergence limit for the optimization itself was 1.0 kcal Å^{−1} mol^{−1}, with use of the Polak–Ribiere conjugate gradient algorithm [23–26].

The spin multiplicity for each cluster assembly was set to “1” for the leucoemeraldine, emeraldine, emeraldine hydrochloride or pernigraniline forms on face-centered cubic Al(100), and set to “3” for all the others. This was done because previous experimental and theoretical evidence suggested that the spin state of all the trimers was a singlet, except for the emeraldine dihydrochloride which

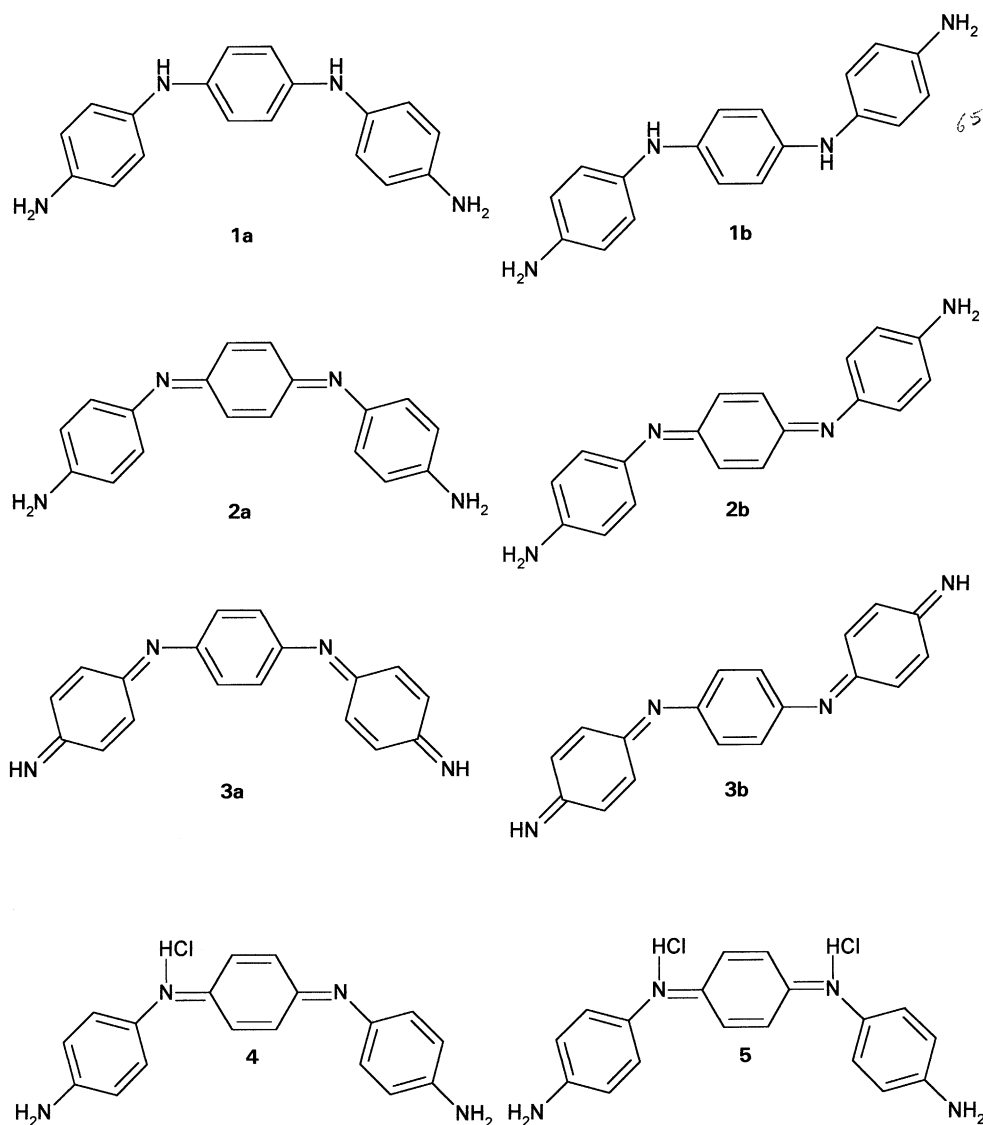


Fig. 1. Redox and conformation forms of aniline trimers.

was a triplet. Though it is possible that the substantial ferromagnetism of the body-centered cubic Fe(100) surface would have resulted in a high multiplicity for each of the trimer/Fe(100) clusters (as noted during Hartree–Fock calculations), no higher multiplicity is available for use with the ZINDO/1 method within the HyperChem suite of programs than a quartet.

Equilibrium constants for electron transfer (ET) reactions were calculated by assumption that, in ET, ΔS is zero, since entropy changes arise primarily from small electronic differences in degenerate states [27]. Therefore, $\Delta H \sim \Delta G = -RT \ln K$.

3. Results and discussion

The thermodynamic considerations necessary to classify aniline oligomers are summarized as follows.

3.1. Aniline trimers as bases

Emeraldine base reacts with 1 mol of hydrogen chloride to form the emeraldine monochloride salt **4** (ES_1).



$$\Delta H_0 = -12.1 \text{ kcal mol}^{-1} - RT = -12.7 \text{ kcal mol}^{-1},$$

$$K_{eq} = 2.1 \times 10^9.$$

Previously published results [6d,7] shows that **4** is a ground state singlet. Further reaction with another mole of hydrogen chloride yields emeraldine dihydrochloride salt **5** (ES_2) which is a ground state triplet. Reaction enthalpies are temperature-dependent, due to the change in the number of molecules (the $p\Delta V$ term).



$$\Delta H_0 = +4.3 - RT = +3.7 \text{ kcal mol}^{-1}, K_{eq} = 1.8 \times 10^{-3}$$

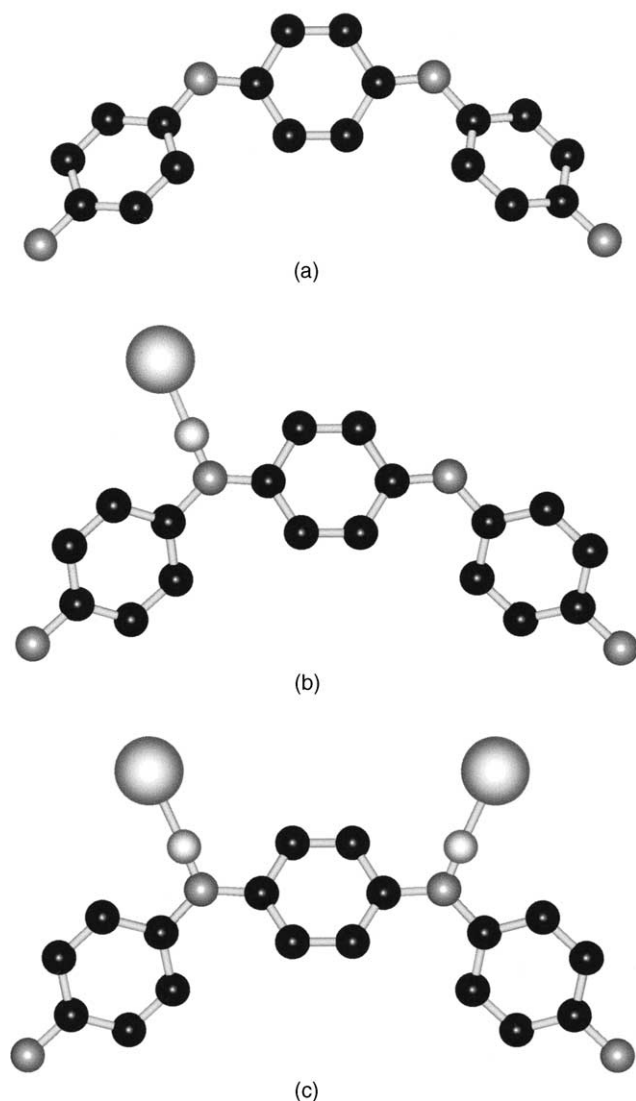


Fig. 2. Molecular structures of aniline trimers, as optimized at B3LYP/6-31G. Carbon atoms are black, nitrogen atoms are grey, chlorine atoms are large white. Hydrogen atoms have been omitted for clarity, except in the hydrochlorides, where the hydrogen atom from the hydrochloride is shown as a small white sphere.

Though the reaction to form the dihydrochloride salt from the monohydrochloride salt is endergonic, the net reaction of EB with HCl to form ${}^3\text{ES}_2$ is exergonic.



$$\Delta H_0 = -7.8 - RT = -9.0 \text{ kcal mol}^{-1}, K_{\text{eq}} = 3.8 \times 10^6.$$

3.2. Enthalpy considerations and the coulomb term in electron transfer

The enthalpy of reaction (ΔH_0) for electron transfer was calculated as the sum of the ionization potential of the donor

$$[\text{IP}(\text{D})] \text{ and the electron affinity of the acceptor } [\text{EA}(\text{A})];^1$$

$$\Delta H_0 = \text{IP}(\text{D}) + \text{EA}(\text{A}) \quad (1)$$

since the enthalpy of the reaction $\text{D} + \text{A} \rightarrow \text{D}^+ + \text{A}^-$ is equal to

$$\begin{aligned} & [\Delta H(\text{D}^+) + \Delta H(\text{A}^-)] - [\Delta H(\text{D}) + \Delta H(\text{A})] \\ &= [\Delta H(\text{D}^+) - \Delta H(\text{D})] + [\Delta H(\text{A}^-) - \Delta H(\text{A})] \\ &= \text{IP}(\text{D}) + \text{EA}(\text{A}), \end{aligned}$$

which is same as the Eq. (1).

Since this neglects the coulombic interaction between the cation and anion formed, the charge transfer enthalpy of reaction at 298 K (ΔH_{CT}) was computed [28] with distance, r equal to 4 Å, which is a reasonable intermolecular distance for stacked aromatic compounds in a crystal [29].

$$\Delta H_{\text{CT}} = \text{IP}(\text{D}) + \text{EA}(\text{A}) - \frac{q^2}{\epsilon r}. \quad (2)$$

Here ϵ is the (static) dielectric constant of the medium (equal to one for a vacuum) and q the charge on an electron. Other effects, such as van der Waals and London forces, chemical bonding, and solvent interactions, have initially been omitted.

3.3. Aniline trimers as donors and acceptors

The redox characteristics of the trimers will determine the limits of their utility in anti-corrosion applications, and therefore must be assessed. The effectiveness of a particular donor or acceptor can be assessed by computation (in default of experimental determination) of the IP or EA. The *smaller* the IP, the better the donor. Similarly, for acceptors, *smaller* the EA (which would mean a more negative enthalpy), better the acceptor.

Koopmans' theorem [17] is often used to estimate the ionization potential of an electron donor, by the approximation that $\text{IP} = -\epsilon_{\text{HOMO}}$. Hoffmann et al. [30] have shown that this approximation is often very poor for hybrid density functionals like B3LYP, though it is better for Hartree–Fock. Similarly, estimations of electron affinity by examination of orbital eigenvalues are often misleading, since Hartree–Fock has HOMO–LUMO gaps that are much too large, and “pure” density functionals (those without any contribution of Hartree–Fock exchange) have gaps that are too small. By either coincidence or design, hybrid functionals like B3LYP are usually within 0.2 eV of the true value of the band gap. The LUMO energy (B3LYP) for both TCNE and TCNQ is ~ -2.02 eV, which implies that they are equally

¹ Note that several sources use a *minus sign* in this equation. This is because the electron affinity is defined somewhat differently. The convention used here is to allow comparison with experimental IPs and EAs as listed in reference [35].

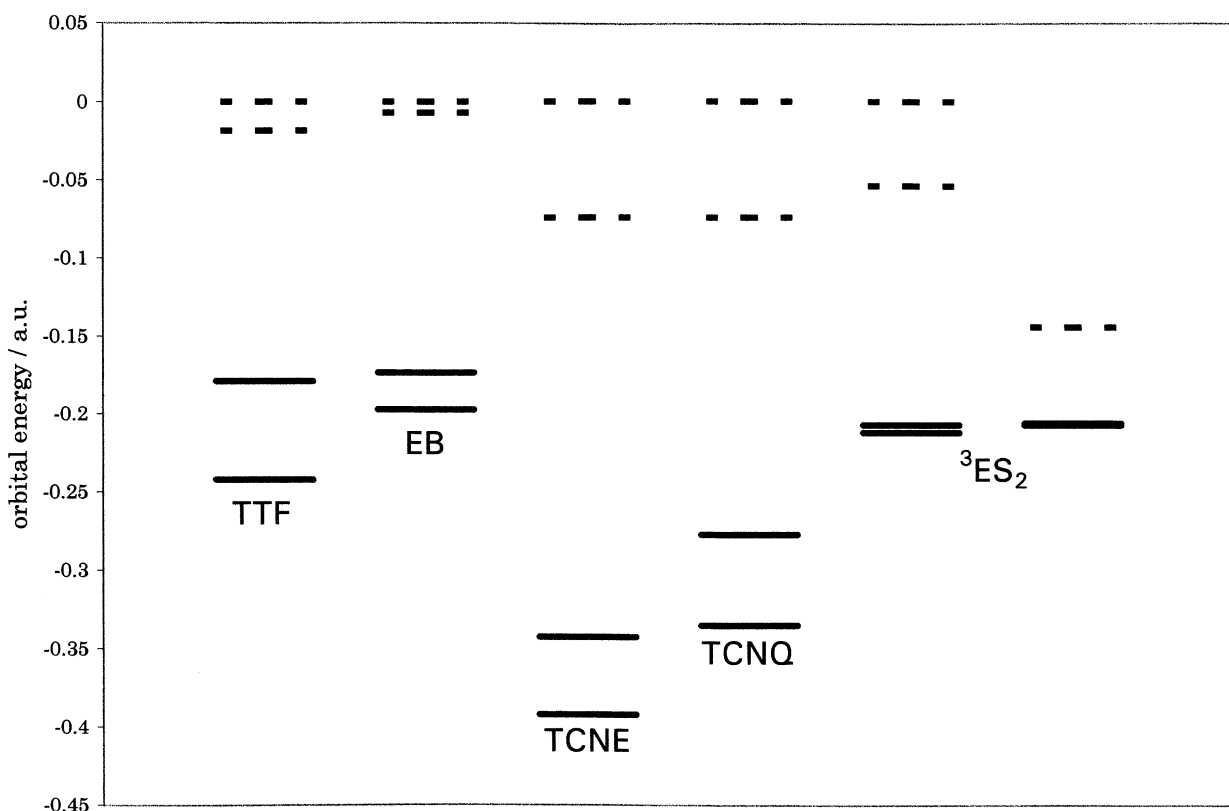
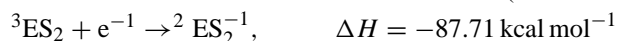
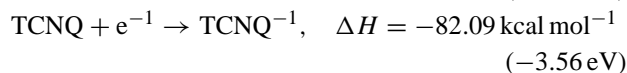
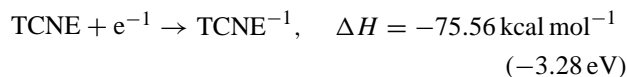
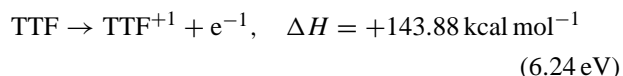


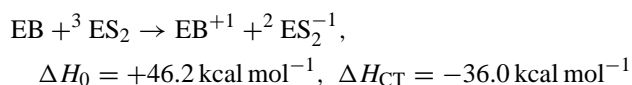
Fig. 3. Frontier orbitals of aniline trimers compared to TTF, TCNE, and TCNQ. Orbital eigenvalues calculated at B3LYP/6-311G(2d,p) on B3LYP/6-31G optimized geometries for the trimers, and B3LYP/6-31G geometries for the others. Occupied orbitals are solid lines, unoccupied orbitals are dashed lines.

strong electron acceptors. However, TCNQ is a stronger acceptor and stronger oxidizing agent than TCNE, and this is correctly found by the method used in this paper.

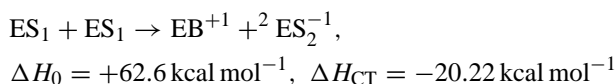
Previous calculations and experiments [6d] have demonstrated that EB is an even more effective electron donor than the prototypical organic donor (TTF). Calculations also suggest that ${}^3\text{ES}_2$ should be an even more effective electron acceptor than acceptor than TCNE or TCNQ. Calculating the IPs and EAs [31–33]:



ES_1 is a more effective electron acceptor than EB, and ${}^3\text{ES}_2$ is the best acceptor of all the emeraldines. It is sufficiently strong to form a charge transfer complex with EB, so long as they are at least as close as 7.1 Å (where $\Delta H_{\text{CT}} = 0$):

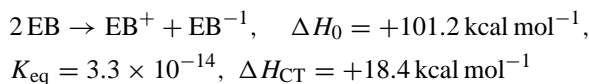


The equilibrium concentration of each salt vis-à-vis the free base is also affected by the reaction



rate-limited by the diffusion of HCl through the matrix. This reaction tends to maximize the concentration of the dihydrochloride salt.

Emeraldine trimer in the base form **3a, b**, (EB) is an effective donor, but a relatively poor acceptor, such that, even at a distance of 4 Å, disproportionation of EB is strongly endergonic.



for the *forward* reaction. The ΔH_0 's for all the emeraldine forms are summarized in Scheme 1.

3.4. Anodic and cathodic reactions of corrosion

To assess corrosion, a trimer/metal model must be examined. Surface iron, modeled as a high spin five atom cluster (Table 3), is a weaker electron donor than EB [34], yet the reaction with ${}^3\text{ES}_2$ is still exergonic at 4.0 Å. Therefore, while the reaction is *favorable* for an atom of iron on the

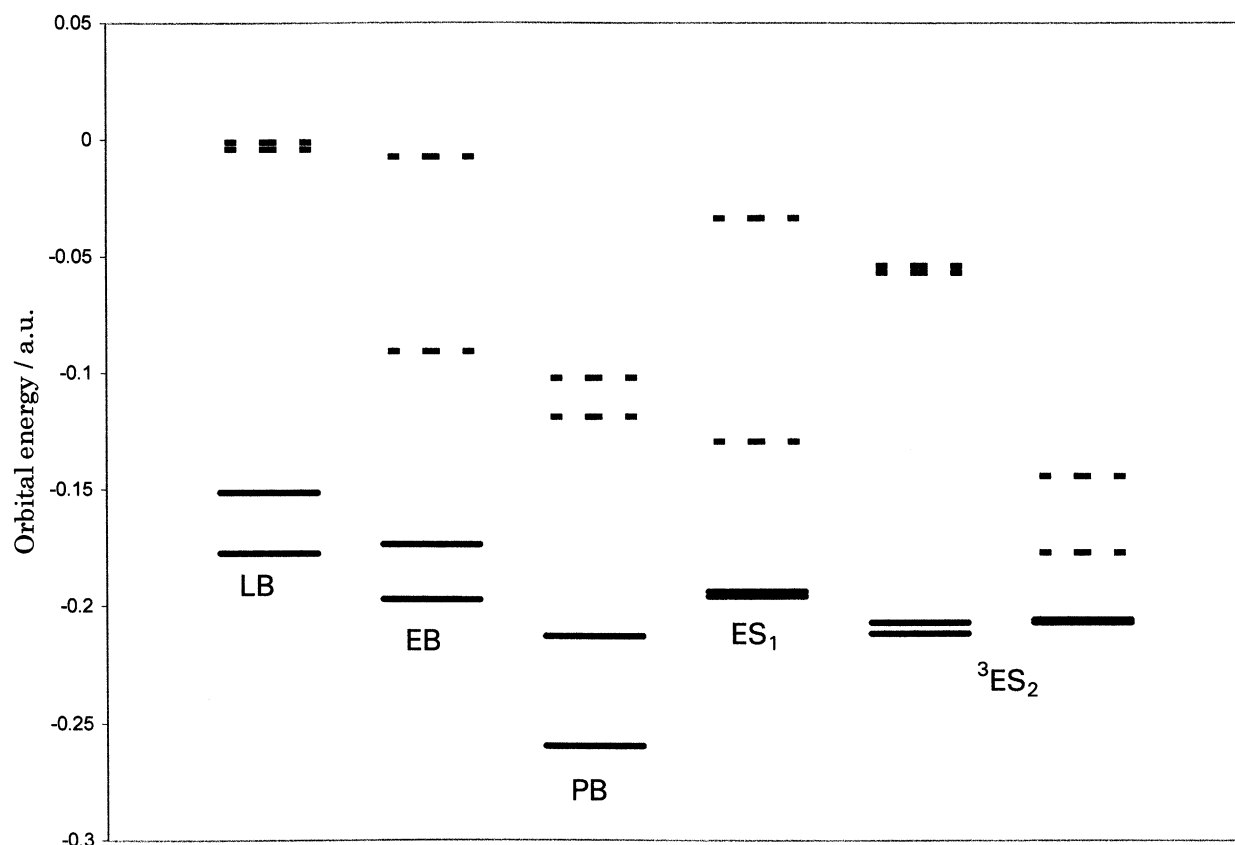
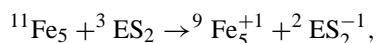


Fig. 4. Frontier orbitals of aniline trimers, calculated at B3LYP/6-311G(2d,p) on B3LYP/6-31G optimized geometries. Occupied orbitals are solid lines, unoccupied orbitals are dashed lines.

surface with a molecule of ${}^3\text{ES}_2$ at the interface, it is *unfavorable* if it involves a reactant *not* at the interface.

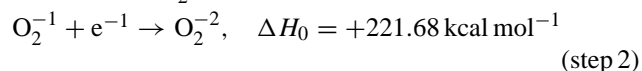
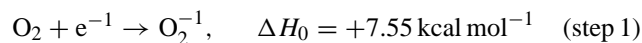


$$\Delta H_0 = +82.29 \text{ kcal mol}^{-1}, \quad \Delta H_{\text{CT}} = -0.53 \text{ kcal mol}^{-1}$$

As, for example, with a iron atom in the bulk, or an ${}^3\text{ES}_2$ several layers from the interface (where $r \gg 4 \text{ \AA}$). Here, this reaction is used to represent the local environment, while ignoring long-ranged effects. Once this complex has formed, the substantial coulomb attraction of the cation for the anion will assist in the adhesion of the protective coating to the surface. A similar reaction of polyaniline with iron has been

reported. [35b] The ${}^2\text{ES}_2^{-1}$ will furthermore, by virtue of its negative charge, repel chloride ions, which are known to anti-passivate iron surfaces [36]. Aluminum [34], though a slightly poorer donator than EB, is a better donator than iron. Therefore, charge transfer will be favored from the aluminum surface to the trimer coating (Table 4).

The reduction of O_2 and O_2^{-1} ;



(or an equivalent pathway via hydrogen peroxide) are important *cathodic* reactions of corrosion; they effectively

Table 3
Spin energies of Fe clusters

Multiplicity	E^a
1	-611.823992
3	-612.087239
5	-612.172014
7	-612.176898
9	-612.263386
11	-612.568867

^a Energies calculated at UHF/LANL2DZ, except for singlet at RHF/LANL2DZ.

Table 4
Energies of adsorption of aniline trimer derivatives on Al(100) and Fe(100) clusters

	Al(100) ^a	Fe(100) ^a
Leucoemeraldine	-416.41	-1833.07
Emeraldine	-472.28	-1836.70
Pernigraniline	-522.28	-2089.07
Emeraldine hydrochloride	-549.32	-2099.90
Emeraldine dihydrochloride	-629.84	-2171.42

^a Energies (in kcal mol⁻¹) as computed using ZINDO/1. No correction was made for zero-point energies.

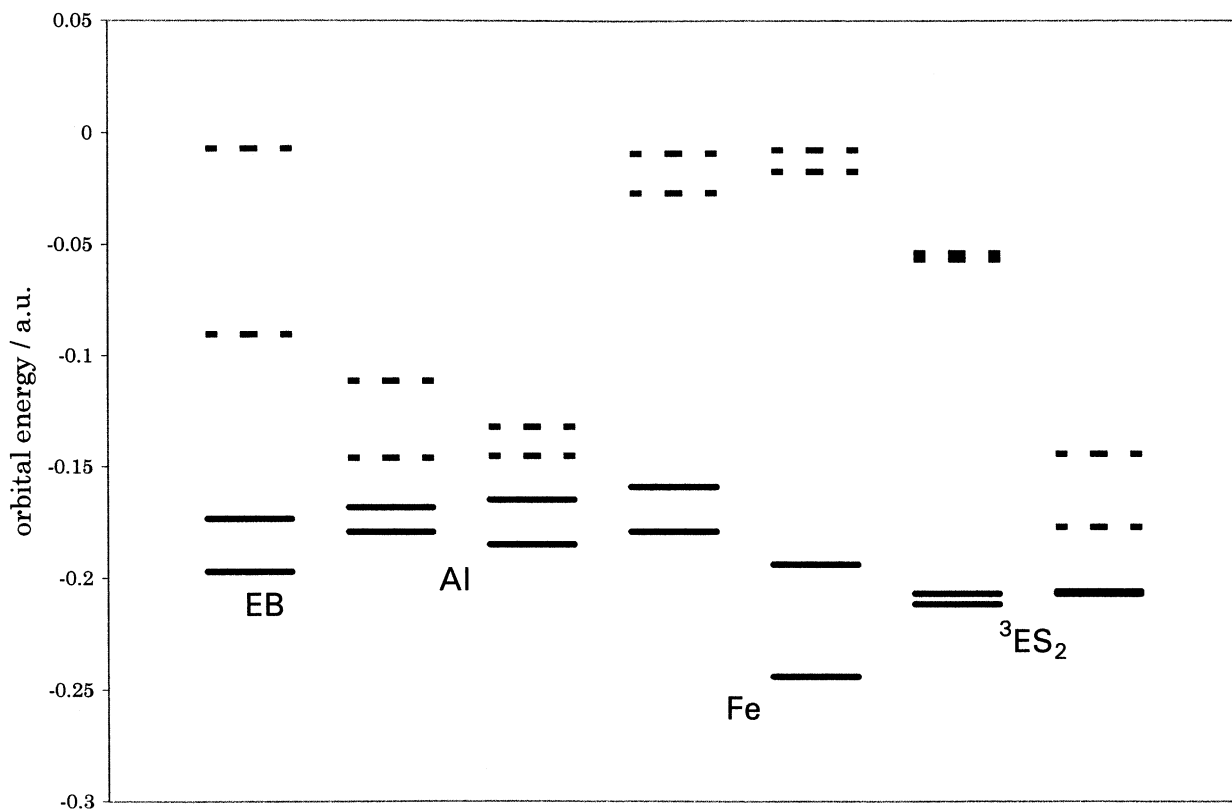


Fig. 5. Frontier orbitals of aniline trimers compared to Al and Fe clusters. Orbital eigenvalues calculated at B3LYP/6-311G(2d,p) on B3LYP/6-31G optimized geometries for the aniline trimers, at B3LYP/6-311G(2d,p) on a constrained crystallographic Al(100) cluster for aluminum, and at UHF/LANL2DZ on a constrained crystallographic Fe(100) cluster for iron. Occupied orbitals are solid lines, unoccupied orbitals are dashed lines.

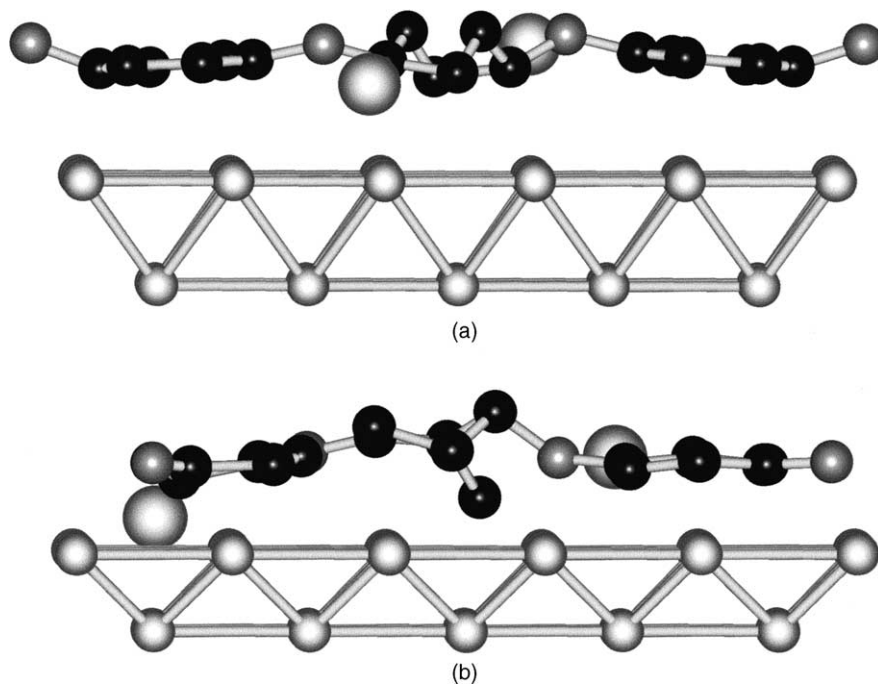
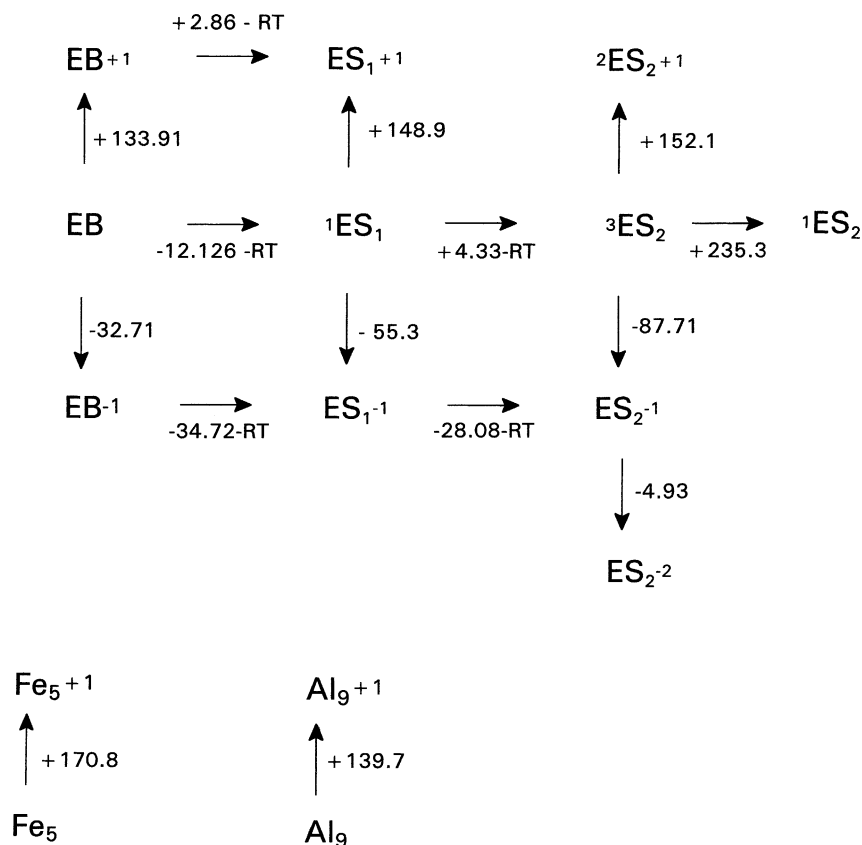


Fig. 6. Molecular structure of emeraldine dihydrochloride absorbed on: (a) Al(100) and (b) Fe(100), as calculated by optimization by ZINDO/1, with each surface constrained to crystallographic coordinates. Color code as in Fig. 2, with the constrained surface the two layers of white spheres in the bottom of each graphic.



All units in kcal mol⁻¹.

Scheme 1. Thermochemical cycle.

constitute a competing charge transfer process. Since step (2) is the rate-determining step, the most significant impact on the cathodic corrosion current comes from attenuation of this step. The ET steps depend on both the distance and the dielectric of the medium. But why do metal surfaces corrode in water, if water has such a large dielectric constant? As, because when the distance is ~ 0 (physisorption of oxygen onto the surface), there are essentially *no* solvent molecules between the donor and the acceptor to minimize the favorable coulomb work term.

3.5. Polarizability and the dielectric constant

Real materials involve multiple deposition of trimer onto metal. If we want to analyze electron transfer through multiple layers of trimer, we need to account for the effective dielectric of the medium, whose effect (as seen in the Rehm–Weller equation) is to decrease the magnitude of the coulombic term. If the dielectric becomes large enough, the coulomb term tends to zero. The dielectric constant ϵ is calculated from the Clausius–Mossotti equation

$$(\epsilon - 1)(\epsilon + 2)^{-1} = \rho P_m M^{-1} \quad (3)$$

where P_m is the molar polarizability (Table 1), ρ the density, and M is the molecular weight.

The polarizability of a molecule is described by a three-dimensional symmetric tensor. If the trimer is so arranged that the central ring is parallel to the xy -plane, and the x -axis runs through the central ring from imine nitrogen to imine nitrogen, the tensor component α_{zz} would apply to electron transfer normal to the central ring. This is the situation if the trimer is absorbed interfacially upon the metal surface. The computed effective dielectric constants are sufficiently close to 1.0 in the zz direction to justify the use of a vacuum permittivity for ET from the surface. In the other directions, the molar polarizabilities are much larger, so much so that in the xx direction, Eq. (3) diverges. This suggests that novel ET phenomena might be investigated by exploiting the large anisotropy of the polarizability.

One can compare the effectiveness of ES as a dielectric with that of the typical coatings [37–39]. Benzene has a dielectric constant of ~ 2.4 , whereas glass ranges from 5–10. Therefore, it appears that ES is not a substantial improvement over other materials that might be used, though it is much better than a simple organic like benzene. Nevertheless, the naturally occurring passive layer that forms on iron

(and steel), is a hydrated iron oxide polymer, of variable composition. It is likely that the addition dielectric effect ($\epsilon = 78.5$) of the bound water is a component of the superior passivation of the “giant polymeric oxide” as compared to $\gamma\text{-Fe}_2\text{O}_3$. It is known that hydrogen-bonding interactions are important in PANi, and it is likely that such interactions are an important reason why aniline trimers offer superior corrosion to PANi. Each PANi chain has equal number of amine (hydrogen-donor) and imine (hydrogen-acceptor) nitrogens, as does each aniline trimer. The imines are unavailable for hydrogen bonding, since they are already bound to hydrogen chloride. The principal difference between the trimer and the polymer, is that in the polymer, each amine nitrogen has *one* hydrogen available for donation, whereas each trimer amine nitrogen has *two* hydrogens available. Nevertheless, in the calculations in this work, the effect of hydrogen-bound water on the dielectric constant of aniline trimers is ignored.

3.6. Adsorption of trimers on aluminum and iron

The idealized absorption geometry of **5** is somewhat unrealistic. To obtain a more accurate geometry of absorption, the various aniline trimers were optimized on each of the Fe(1 0 0) and Al(1 0 0) surfaces, where the extended surfaces were modeled by a 28 atom cluster (Fig. 6). Though the calculated energies of absorption are probably greatly exaggerated, the general trends suggest that the more *oxidized* the trimer, the *stronger* the binding to the surface. Chemical bonding interactions are probably not negligible, as assumed in the simple charge transfer model described above. Using the same geometry as optimized by ZINDO/1 for **5**, but a more truncated 8 atom surface model cluster, we calculated the single point energy of the assembly at B3LYP/6-31G+. The sum of the partial charges on the aluminum atoms ~ 1 , which indicates that there is a net loss of one electron from the aluminum surface to **5**.

This calculation also provides an estimate for V , the electronic coupling between the surface and the trimer during charge transfer. V was estimated [40] as one-half of the difference between the eigenvalues of the HOMO and the HOMO-1. Since $V \sim 9.4 \text{ kcal mol}^{-1}$ for the aluminum surface with **5**, $V \gg k_B T$, which confirms that the electron transfer reaction is strongly adiabatic. For the reaction on the iron surface, $V \sim 9.7 \text{ kcal mol}^{-1}$. For electron transfer between **2a** and **5**, $V = 1.9 \text{ kcal mol}^{-1}$, but for transfer between **5** and **5**, V is only $0.4 \text{ kcal mol}^{-1}$, which is less than $k_B T$, so it is non-adiabatic.

3.7. Effect of oxide layers and defects

The model herein presented is still somewhat too simple-minded in that it ignores the ubiquitous oxide layers. While it should be possible to clean an iron surface and deposit a coating of organic with minimal formation of iron oxide (due to kinetic factors), it is certainly impossible to say the same for aluminum. In what ways will the

oxide coating affect electron transfer? The first effect can be estimated by modeling the oxide as a simple dielectric medium. If the oxide is hematite ($\alpha\text{-Fe}_2\text{O}_3$), $\epsilon = 25.0$; if it is goethite ($\alpha\text{-FeOOH}$), $\epsilon = 11.7$ [41]. If magnetite (Fe_3O_4) has formed, the surface, at least in the magnetite region, can not be modeled as a dielectric at all, since magnetite is conductive. Corundum ($\alpha\text{-Al}_2\text{O}_3$) has a dielectric constant of 10.43. The Marcus theory derived rate constants below can be corrected by assuming two electron transfers, the first from the metal to the polymer through the oxide, and the second from the oxide–polymer interface to the surface, through the polymer. An accurate calculation is dependent on knowledge of the oxide layer thickness.

There is also a difficulty that the ZINDO/1 calculation involves the binding of oligomer to the metal surfaces, when in fact it is most likely to be binding to an oxide layer. Fortunately, $\alpha\text{-Fe}_2\text{O}_3$ (at least 0001) is iron-terminated, and $\alpha\text{-Al}_2\text{O}_3$ is aluminum-terminated [41]. Therefore, at the interface, within the accuracy of a semi-empirical calculation, the calculated geometries of the oligomers might be expected to not change substantially from what they would be on an oxide layer.

A final difficulty of the proposed model is that the effects of defects are not specifically addressed. Frequently in catalysis, essentially all the reactions take place at defect sites. We suspect that the effect of defects in the binding of aniline oligomers to the metal surface is minimized by the very large surface area of the oligomer, which essentially interacts with a large “generalized” area of the surface, whose effects can be reliably modeled as an average of defect and non-defect sites.

3.8. Calculation of electron transfer rates

We calculate the free energy of activation of electron transfer ΔG^* (in the case of strong coupling) by [42]

$$\Delta G^* = 0.25\lambda - V + V^2\lambda^{-1} \quad (4)$$

and by

$$\Delta G^* = \frac{1}{2}\lambda \quad (5)$$

for the nonadiabatic case. Then the rate of electron transfer is

$$k_{\text{ET}} = k_B T h^{-1} \exp\left(\frac{-\Delta G^*}{RT}\right). \quad (6)$$

The internal reorganization of the reactants λ_{in} was computed by the CNG (cation in neutral geometry) method [43,44].

$$\lambda_{\text{in}} = \Delta H\{c^0\} - \Delta H\{c^{+1}\} + \Delta H\{n^{+1}\} - \Delta H\{n^0\} \quad (7)$$

where $\Delta H\{c^{+1}\}$ is the enthalpy of the optimized cation, $\Delta H\{n^0\}$ the enthalpy of the optimized neutral molecule, $\Delta H\{c^0\}$ the enthalpy of the neutral in the optimized geometry of the cation, and $\Delta H\{n^{+1}\}$ the enthalpy of the cation

in the optimized geometry of the neutral molecule. We find, $\lambda_{\text{in}} = 9.5$ kcal for **2a**.

Similarly, for an anion,

$$\lambda_{\text{in}} = \Delta H\{a^0\} - \Delta H\{a^{-1}\} + \Delta H\{n^{-1}\} - \Delta H\{n^0\} \quad (8)$$

where $\Delta H\{a^{-1}\}$ is the enthalpy of the optimized *anion*, $\Delta H\{n^0\}$ the enthalpy of the optimized neutral molecule, $\Delta H\{a^0\}$ the enthalpy of the neutral in the optimized geometry of the *anion*, and $\Delta H\{n^{-1}\}$ the enthalpy of the *anion* in the optimized geometry of the neutral molecule. For **5**, we get, $\lambda_{\text{in}} = 7.8$ kcal mol⁻¹. Since we chosen to calculate the IPs of the metal clusters with fixed crystallographic coordinates, we set $\lambda_{\text{in}} = 0$ for the clusters.

In the case of electron transfer from ²ES₂⁻¹ (call it molecule, a), to ³ES₂ (molecule, b), the products are ³ES₂ (molecule, a) and ²ES₂⁻¹ (molecule b). There is no internal reorganization since the effect of the reaction is simply a renaming of the two molecules. There is also no coulomb work term. The energy of energy of activation for ET is determined solely by the outer (solvent) reorganization term.

The outer (solvent) reorganization energy is

$$\lambda_{\text{out}} = q^2 g(r, d) \gamma \quad (9)$$

where q is the electron charge, $g(r, d)$ the distance between the ions, and γ the solvent parameter. $g(r, d)$ is approximated by the expression $[(2r_A)^{-1} + (2r_B)^{-1} - d^{-1}]$ with r_A, r_B being the radii of ions, and d the distance between the two redox centers. Since the surface is essential non-solvated, solvent reorganization effects are dominated by the electronic double layer. At the limit of the transfer of a single electron, the effect should be vanishingly small. We set the $(2r_A)^{-1}$ term equal to zero, effectively making the “radius” of the surface infinitely large. For the radius of either EB or ³ES₂, we note that, in the z direction, the distance across the molecule is 1.5 Å, so we set the “radius” to 0.75 Å. Another technique would have been to calculate the molecular volume (1028.47 Å³ for ³ES₂ by the *ChemPlus* add-on to HyperChem), and then, making the assumption that the ion is spherical, calculate the radius. This method yields a radius of 9.2 Å, which is twice as large as the distance, thereby making $g(r, d)$ negative. We therefore set the radius to 0.75 Å as a more reasonable solution.

$$\gamma = (\varepsilon_{\text{opt}})^{-1} - (\varepsilon_a)^{-1} \quad (10)$$

Usually, ε_{opt} is the square of the refractive index n_D . Since n_D is unknown for the aniline trimers, we estimate it as the n_D of aniline (1.5824) [45].

The total reorganization energy of ET is $\lambda = \lambda_{\text{in}} + \lambda_{\text{out}} + \lambda_{\text{so}}$, where λ_{so} is a spin-orbital coupling term, which is likely to be insignificant for the trimers themselves and for aluminum, but could become important for iron. In this paper, spin-orbit coupling is considered to be insignificant in comparison with the very large electronic coupling.

ET from the surfaces to the trimers is ultra-fast (Table 5). This is a consequence of the very strong coupling, and

Table 5
Marcus parameters for aniline trimers

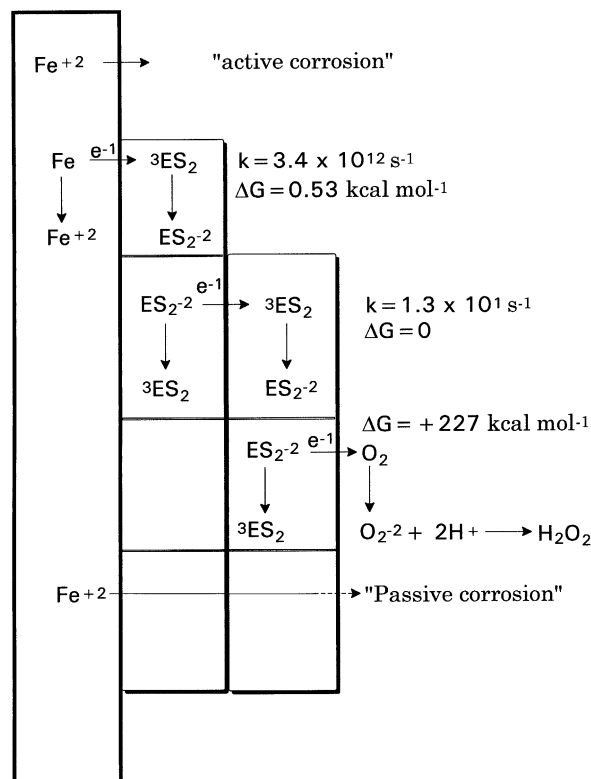
Donor	Acceptor	V ^a	λ_{in}^a	λ_{out}^a	G ^{*a}	k _{ET} ^b
Al	³ ES ₂	9.4	7.8	0.00	3.88	9.4 × 10 ¹⁰
		9.4	7.8	27.02	1.88	2.6 × 10 ¹²
Fe	³ ES ₂	9.7	7.8	0.00	4.31	4.7 × 10 ¹⁰
		9.7	7.8	27.02	1.75	3.4 × 10 ¹²
EB	³ ES ₂	1.9	17.3	0.00	2.63	7.7 × 10 ¹¹
		1.9	17.3	70.26	20.03	2.0 × 10 ⁻¹
³ ES ₂	³ ES ₂	0.4	0.0	0.00	0.00	6.2 × 10 ¹²
		0.4	0.0	70.26	17.57	1.3 × 10 ⁻¹

^a kcal mol⁻¹.

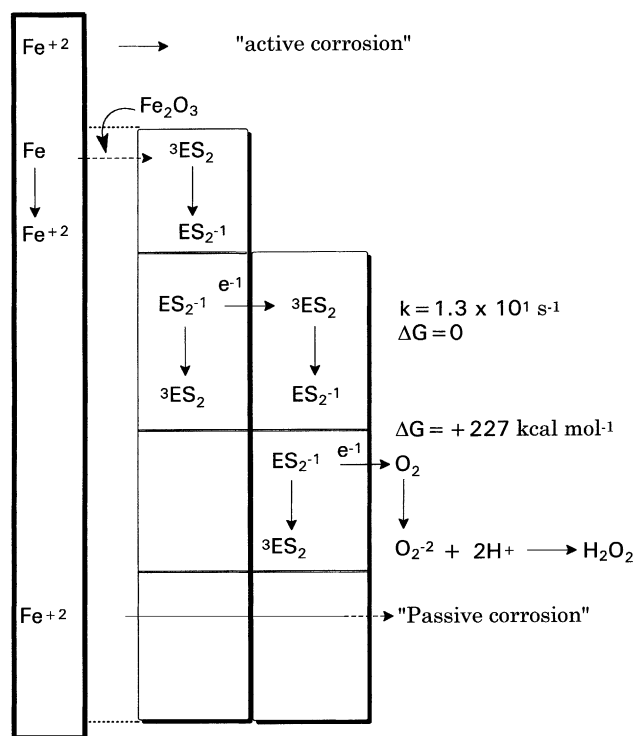
^b s⁻¹.

the modest size of the reorganization energy. Experimental studies on intervalence charge-transfer complexes, similarly composed of aniline units, found equivalent rates [40]. Rates of ET are much faster from the metal surfaces to the trimer, than from one trimer to another. This is, in essence, one method of minimization of the *active* cathodic current. Another way to think of this is to consider the trimer layer as an *electron buffer*.

The *passive* corrosion current, the net migration of the positively charged ferrous/ferric ion through the polymer overlayer, is inhibited by the negative charge on the polymer molecules. (The *active* corrosion current is inhibited by the barrier effect, and by the electrochemical effects on the cathodic and anodic reactions.) This negative charge



Scheme 2. Electron transfer between surface and trimers.



Scheme 3. Electron transfer among surface, oxide layer, and trimers.

will eventually “leak” out to oxygen dissolved in the solution. The rate of this leakage will be dependant on the concentration of oxygen in the solution, which will itself depend upon, among other things, temperature (Hadley’s law). The leakage of electrons will reoxidize ${}^2\text{ES}_2^{-1}$ to ${}^3\text{ES}_2$ (Schemes 2 and 3). This effect has been investigated at elevated temperatures in air [35b], where the concentration of O_2 is, of course, much higher than in solution.

The primary effect of pH will be on the equilibrium concentration of ES_2 versus EB. At higher pH, attack by OH^{-1} will displace Cl^{-1} , to form a hydrogen-bound complex of EB and water, which is ineffective at corrosion inhibition, because of the poorer electron accepting properties of EB. This accounts for the superior inhibition performance of both PANi and the trimer in acid media, as compared to neutral or alkaline media. While there are certain pH effects in the free energy change of the reduction of dioxygen (the protonation of O_2^{-2} to form H_2O_2), these effects are expected to be essentially the same for all organic protective coatings.

4. Conclusions

The calculation of thermochemical properties of aniline trimers in various oxidation states, in conjunction with similar calculations on cluster models of iron and aluminum surfaces, has shown that the emeraldine dihydrochloride is the most effective form for corrosion inhibition. The transfer of electrons from the surface to the trimer is energetically favorable (and kinetically fast) at the trimer/surface interface. The

oxidized metal atoms at the surface are inhibited from dissolution by the coulombic interaction with the trimer layer. As charge builds up at the polymer interface, it migrates very slowly toward the trimer/air or trimer/water interface. The electrons are eventually transferred to dioxygen; though this reaction is energetically unfavored, the high relative concentration of oxygen at the trimer boundary drives the reaction. The reaction is made even more thermodynamically unfavored by the dielectric effect of the trimer, which minimizes the favorable coulomb term. Thus, a model for corrosion inhibition by aniline trimers, based on the analysis of both equilibrium (thermodynamics and potentials) and rate (kinetics), is advanced with the support of density functional theory (DFT).

Acknowledgements

We gratefully acknowledge the National Science Foundation (grant DMR990003P) for support. L.T.S. thanks the Graduate School of Temple University for a dissertation completion fellowship.

References

- [1] (a) A.G. MacDiarmid, Y. Min, K. Kaneto, M. Kaneko, *Synth. Met.* 71 (1995) 2211; (b) M. Angelopoulos, R. Dipietro, W.G. Zheng, A.G. MacDiarmid, A.J. Epstein, *Synth. Met.* 84 (1997) 35; (c) J. Joo, A.J. Epstein, E.J. Oh, G. Min, A.G. MacDiarmid, *Synth. Met.* 69 (1995) 251; (d) G. Du, A.J. Epstein, J. Avlyanov, K.G. Reimer, C.Y. Wu, A. Benatar, A.G. MacDiarmid, *Synth. Met.* 85 (1997) 1339; (e) R.S. Kohlman, D.B. Tanner, G.G. Ihas, Y.G. Min, A.G. MacDiarmid, A.J. Epstein, *Synth. Met.* 84 (1997) 709; (f) R.S. Kohlman, Y. Min, A.G. MacDiarmid, A.J. Epstein, *Synth. Met.* 69 (1995) 211; (g) J.P. Pouget, C.-H. Hsu, A.G. MacDiarmid, A.J. Epstein, *Synth. Met.* 69 (1995) 119.
- [2] (a) H.L. Wang, F. Huang, A.G. MacDiarmid, Y.Z. Wang, D.D. Gebler, A.J. Epstein, *Synth. Met.* 80 (1996) 97; (b) H.L. Wang, A.G. MacDiarmid, Y.Z. Wang, D.D. Gebler, A.J. Epstein, *Synth. Met.* 78 (1996) 33; (c) F. Huang, H.L. Wang, M. Feldstein, A.G. MacDiarmid, B.R. Hsieh, A.J. Epstein, *Synth. Met.* 85 (1997) 1283.
- [3] P. Novak, K. Mueller, K.S.V. Santhanam, O. Haas, *Chem. Rev.* 97 (1997) 207.
- [4] (a) N. Ahmad, A.G. MacDiarmid, *Synth. Met.* 78 (1996) 103; (b) L.T. Sein, Jr., L. Levarity, R. Keyer, S.A. Jansen, Y. Wei, *Polyanilines as alternative anti-corrosion materials: a molecular level model of the corrosion process*, in: G. Wnek, D.J. Trantolo, T.M. Cooper, J.D. Oresser (Eds.), *Electr. Opt. Polym.*, Marcel Dekker, New York, 1997, p. 1; (c) R. Vallerio, R. Keyer, S. Grabania, M. Landis, S.A. Jansen, Y. Wei, *Assessment of polyanilines as alternative anti-corrosion materials: a theoretical analysis of metal-polymer adhesion*, in: A.K.-Y. Jen, C.Y.-C. Lee, L.R. Dalton, M.F. Rubner, G.E. Wnek, L.Y. Chiang (Eds.), *Electr. Opt. Mag. Prop. Org. Solid State Mater. III*, Materials Research Society, Pittsburgh, PA, 1996; (d) L.T. Sein Jr., S. Kolla, P. Pasupaleti, K. Patel, S.A. Jansen, Y. Wei, *Polymer Preprints, Am. Chem. Soc., Div. Polym. Chem.* 39 (1998) 117.

- [5] (a) S.M. Long, R.S. Kohlman, A.J. Epstein, K.R. Brennehan, A. Sapirigin, M. Angelopoulos, S.L. Buchwalter, A. Rossi, W. Zheng, A.G. MacDiarmid, *Synth. Met.* 84 (1997) 809;
 (b) J. Joo, Y.C. Chung, H.G. Song, J.S. Baeck, W.P. Lee, A.J. Epstein, A.G. MacDiarmid, S.K. Jeong, E.J. Oh, *Synth. Met.* 84 (1997) 739;
 (c) A. Sapirigin, A.J. Epstein, R.S. Kohlman, S.M. Long, M. Angelopoulos, Y.-H. Liao, A.G. MacDiarmid, W. Zheng, K.R. Brennehan, *Synth. Met.* 84 (1997) 767;
 (d) L.H.C. Mattoso, G.L. Mantovani, A.G. MacDiarmid, *Synth. Met.* 84 (1997) 73;
 (e) A.G. MacDiarmid, A.J. Epstein, *Synth. Met.* 69 (1995) 85.
- [6] (a) A.G. MacDiarmid, Y. Zhou, J. Feng, *Synth. Met.* 100 (1999) 131;
 (b) W.J. Zhang, J. Feng, A.G. MacDiarmid, A.J. Epstein, *Synth. Met.* 84 (1997) 119;
 (c) J.P. Sadighi, R.A. Singer, S.L. Buchwald, *J. Am. Chem. Soc.* 120 (1998) 4960;
 (d) L.T. Sein Jr., T. Duong, A. Major, Y. Wei, S.A. Jansen, *J. Mol. Struct. (Theochem)* 37 (2000) 498;
 (e) L.T. Sein Jr., T. Duong, Y. Wei, S.A. Jansen, *Synth. Met.* 113 (2000) 145.
- [7] S.A. Jansen, T. Duong, A. Major, Y. Wei, L.T. Sein Jr., *Synth. Met.* 105 (1999) 107.
- [8] (a) C. Yang, G. Wei, G. Feng, Y. Wei, *Synth. Met.* 84 (1997) 289;
 (b) J.M. Yeh, Doctoral dissertation, Drexel University, 1996;
 (c) Y. Wei, W. Wang, J.M. Yeh, B. Wang, D. Yang, J.K. Murray, D. Jin, G. Wei, *G. Am. Chem. Soc. Ser. No. 585*, 1995, Chapter 11, 125.
- [9] Unpublished results.
- [10] (a) X.-L. Wei, M. Fahlman, A.J. Epstein, *Macromol.* 32 (1999) 3114;
 (b) M.J. Winokur, B.R. Mattes, *Macromol.* 31 (1998) 8183;
 (c) J. Stejskal, I. Sapurina, M. Trchova, J. Prokes, I. Krivka, E. Tobolkova, *Macromol.* 31 (1998) 2218;
 (d) I. Kulszewicz-Bajer, I. Wielgus, A. Pron, P. Rannou, *Macromol.* 30 (1997) 7091;
 (e) M.P. Espe, B.R. Mattes, J. Schaefer, *Macromol.* 30 (1997) 6307;
 (f) W. Zheng, M. Angelopoulos, A.J. Epstein, A.G. MacDiarmid, *Macromol.* 30 (1997) 2953;
 (g) J.A. Conklin, M.R. Anderson, H. Reiss, R.B. Kaner, *J. Phys. Chem.* 100 (1996) 8425.
- [11] S. Patai, (Ed.), *The Chemistry of the Carbon-Nitrogen Double Bond*. Interscience Publishers, London, 1970.
- [12] Gaussian 94 (Revision D.1), M.J. Frisch, G.W. Trucks, H.B. Schiegel, P.M.W. Gill, B.G. Johnson, M.A. Robb, J.R. Cheeseman, T.A. Keith, G.A. Petersson, J.A. Montgomery, K. Raghavachari, M.A. Al-Laham, V.G. Zakrzewski, J.V. Ortiz, J.B. Foresman, C.Y. Peng, P.Y. Ayala, M.W. Wong, J.L. Andres, E.S. Replogle, R. Gomperts, R.L. Martin, D.J. Fox, J.S. Binkley, D.J. Defrees, J. Baker, J.P. Stewart, M. Head-Gordon, C. Gonzalez, J.A. Pople, Gaussian Inc., Pittsburgh, PA, 1995.
- [13] (a) A.D. Becke, *J. Chem. Phys.* 98 (1993) 5648;
 C. Lee, W. Yang, R.G. Parr, *Phys. Rev. B* 37 (1988) 785.
- [14] P.J. Hay, W.R. Wadt, *J. Chem. Phys.* 82 (1985) 284.
- [15] (a) G.A. Petersson, M.A. Al-Laham, *J. Chem. Phys.* 94 (1991) 6081;
 (b) G.A. Petersson, A. Bennett, T.G. Tensfeldt, M.A. Al-Laham, W.A. Shirley, J. Mantzaris, *J. Chem. Phys.* 89 (1988) 2193.
- [16] J.B. Foresman, A. Frisch. *Exploring Chemistry with Electronic Structure Methods*, second ed., Gaussian Inc., Pittsburgh, PA, 1996.
- [17] T. Koopmans, *Physica I* (1934) 104.
- [18] T. Tsunekawa, K. Yamaguchi, *J. Phys. Chem.* 96 (1992) 10268.
- [19] R. Cammi, B. Mennucci, J. Tomasi, *J. Am. Chem. Soc.* 120 (1998) 8834.
- [20] (a) A.D. Bacon, M.C. Zerner, *Theor. Chim. Acta* 53 (1979) 21;
 (b) M.C. Zerner, G.H. Loew, R.F. Kirchner, U.T. Mueller-Westerhoff, *J. Am. Chem. Soc.* 102 (1980) 589;
 (c) W.P. Anderson, W.D. Edwards, M.C. Zerner, *Inorg. Chem.* 25 (1986) 2728;
 (d) J.C. Culberson, P. Knappe, N. Rosch, M.C. Zerner, *Theoret. Chem. Acta* 71 (1987) 21;
 (e) J.D. Baker, M.C. Zerner, *J. Phys. Chem.* 94 (1990) 2866;
 (f) W. Anderson, T. Cundari, M.C. Zerner, *Int. J. Quantum Chem.* 39 (1990) 31;
 (g) W. Anderson, T. Cundari, R. Drago, M.C. Zerner, *Inorg. Chem.* 29 (1991) 1.
- [21] HyperChem, version 4.0, HyperChem is a registered trademark of HyperCube Inc., Waterloo, Canada.
- [22] (a) P. Pulay, G. Fogarasi, F. Pang, J.E. Boggs, *J. Am. Chem. Soc.* 101 (1979) 2550;
 (b) P. Pulay, G. Fogarasi, *J. Chem. Phys.* 96 (1992) 2856.
- [23] E. Polak, G. Ribiere, *G. Rev. Fr. Inf. Rech. Oper.* 16-R1 (1969) 35.
- [24] R. Fletcher, C.M. Reeves, *J. Comp. 7* (1964) 149.
- [25] R. Fletcher. *Practical Methods of Optimization*, second ed., Wiley, Tiptree, Essex, UK, 1987.
- [26] H. Mukai, *Math. Program.* 7 (1979) 298.
- [27] R.A. Marcus, *J. Chem. Phys.* 24 (1956) 966.
- [28] D. Rehm, A. Weller, *Isr. J. Chem.* 8 (1970) 259.
- [29] The compound α,α' -bis(dithieno[3,2-*b*:2',3'-*d*]thiophene) {BDT}, has an interlayer distance of 3.557 Å, X.-C. Li, H. Siringhaus, F. Garnier, A.B. Holmes, S.C. Moratti, N. Feeder, W. Clegg, S.J. Teat, R.H. Friend, *J. Am. Chem. Soc.* 120 (1998) 2206.
- [30] R. Stowasser, R. Hoffmann, *J. Am. Chem. Soc.* 121 (1999) 3414.
- [31] IP of TTF is 6.26 eV S. Horiuchi, H. Yamochi, G. Saito, K. Sakaguchi, M. Kusunoki, *J. Am. Chem. Soc.* 118 (1996) 8604.
- [32] A high electron affinity (EA = -3.17 ± 0.2 eV) makes TCNE a good oxidizing agent, S. Chowdhury, P. Kebarle, *P.J. Am. Chem. Soc.* 108 (1986) 5453.
- [33] EA of TCNQ is -3.3 ± 0.3 eV C. Jin, R.E. Hauffer, R.L. Hettich, C.M. Basich, R.N. Compton, A.A. Puzetzy, A.V. Demyanenko, A.A. Tuinman, *Science* 263 (1994) 68.
- [34] IP of Al is 138 kcal mol⁻¹ (577.4 kJ mol⁻¹); IP of iron is 759.3 kJ (181.5 kcal mol⁻¹), J. Emsley, *The Elements*, second ed., Oxford University Press, Oxford, 1991.
- [35] (a) M. Lira-cantu, P. Gomez-Romero, *Chem. Mater.* 10 (1998) 698;
 (b) B.C. Beard, P. Spellane, *Chem. Mater.* 9 (1997) 1949;
 (c) M. Higuchi, D. Imoda, T. Hirao, *Macromol.* 29 (1996) 8277;
 (d) T. Tatsuma, H. Matsui, E. Shouji, N. Oyama, *J. Phys. Chem.* 100 (1996) 14016.
- [36] J.O'M. Bockris, B. Rubin, A.R. Despic, B. Lovrecik, *Electrochim. Acta* 17 (1972) 973.
- [37] (a) G.P. Wiederrecht, W.A. Svec, M.R. Wasielewski, *J. Am. Chem. Soc.* 119 (1997) 6199;
 (b) G.P. Wiederrecht, B.A. Yoon, W.A. Svec, M.R. Wasielewski, *J. Am. Chem. Soc.* 119 (1997) 3358.
- [38] T. Simonson, C.L. Brooks III, *J. Am. Chem. Soc.* 118 (1996) 8452.
- [39] In proteins, the aromatic amino acids tyrosine, phenylalanine, and tryptophan "play a role similar to polarizable solvents," H. Housjou, Y. Inoue, M. Sakurai, *J. Am. Chem. Soc.* 120 (1998) 4459.
- [40] C. Lambert, G. Nöll, *J. Am. Chem. Soc.* 121 (1999) 8434.
- [41] G.E. Brown Jr., V.E. Henrich, W.H. Casey, D.L. Clark, C. Eggleston, A. Felmy, D.W. Goodman, M. Graetzel, G. Maciel, M.I. McCarthy, K.H. Nealson, D.A. Sverjensky, M.F. Toney, J.M. Zachara, *Chem. Rev.* 99 (1999) 77.
- [42] (a) N. Sutin, *Prog. Inorg. Chem.* 30 (1983) 441;
 (b) C. Creutz, M.D. Newton, N. Sutin, *J. Photochem. Photobiol. A* 82 (1994) 47.
- [43] S.F. Nelsen, H. Chang, J.J. Wolff, J. Adamus, *J. Am. Chem. Soc.* 115 (1993) 12276.
- [44] S.F. Nelsen, S.C. Blackstock, Y. Kim, *J. Am. Chem. Soc.* 109 (1987) 677.
- [45] Other representative refractive indices for polymers: 1.490 (PMMA), 1.577 (methyl phenyl sulfoxide), 1.35 (PTFE) G. Pan, A.S. Tse, R. Kesavamoorthy, S.A. Asher. *J. Am. Chem. Soc.* 120 (1998) 6518.